Steinernema tarimense n. sp. (Rhabditida: Steinernematidae), a new entomopathogenic nematode from Tarim Basin, Xinjiang, China

F. Zhan[1,2] ⓘ, C. Tian[3] ⓘ, H. Li[4], R. Yang[2], H. Bao[2], S. Zhang[2], X. Zhang[2], Y. Shi[2], M. Tomalak[5], V. Půža[6] and W. Guo[7] ⓘ

[1]College of Life Sciences and Technology, Xinjiang University, Urumqi, Xinjiang 830046, China; [2]Institute of Microbiology, Xinjiang Academy of Agricultural Sciences, Xinjiang Key Laboratory of Special Environmental Microbiology, Urumqi, Xinjiang 830091, China; [3]Institute of Plant Protection, Jilin Academy of Agricultural Sciences, Changchun 130033, China; [4]Department of Plant Pathology, College of Plant Protection, Nanjing Agricultural University, Nanjing 210095, China; [5]Department of Biological Pest Control, Institute of Plant Protection, Władysława Wegorka 20, 60-318 Poznan, Poland; [6]Laboratory of Insect Pathology, Institute of Entomology, Czech Academy of Sciences, Branišovská 31, 370 05 České Budějovice, Czech Republic and [7]Institute of Plant Protection, Xinjiang Academy of Agricultural Sciences/ Xinjiang Key Laboratory of Agricultural Biosafety, Urumqi 830091, China

Abstract

A novel entomopathogenic nematode (EPN) species, *Steinernema tarimense* n. sp., was isolated from soil samples collected in a *Populus euphratica* forest located in Yuli County within the Tarim Basin of Xinjiang, China. Integrated morphological and molecular analyses consistently place *S. tarimense* n. sp. within the '*kushidai*-clade'. The infective juvenile (IJ) of new species is characterized by a body length of 674–1010 μm, excretory pore located 53–80 μm from anterior end, nerve ring positioned 85–131 μm from anterior end, pharynx base situated 111–162 μm from anterior end, a tail length of 41–56 μm, and the ratios D% = 42.0–66.6, E% = 116.2–184.4, and H% = 25.5–45.1. The first-generation male of the new species is characterized by a curved spicule length of 61–89 μm, gubernaculum length of 41–58 μm, and ratios D% = 36.8–66.2, SW% = 117.0–206.1, and GS% = 54.8–82.0. Additionally, the tail of first-generation female is conoid with a minute mucron. Phylogenetic analyses of ITS, 28S, and *mt12S* sequences demonstrated that the three isolates of *S. tarimense* n. sp. are conspecific and form a sister clade to members of the '*kushidai*-clade' including *S. akhursti*, *S. anantnagense*, *S. kushidai*, and *S. populi*. Notably, the IJs of the new species exhibited faster development at 25°C compared to other *Steinernema* species. This represents the first described of an indigenous EPN species from Xinjiang, suggesting its potential as a novel biocontrol agent against local pests.

Introduction

Entomopathogenic nematodes (EPNs) are important biological control agents for pests in natural ecosystems. These nematodes, primarily represented by *Steinernema* and *Heterorhabditis* species, exhibit remarkable host-seeking capabilities, entering insect hosts through natural openings (mouth, anus) or integumentary wounds (Stuart *et al.* 2006). They not only effectively suppress pest populations and mitigate crop losses, but also substantially reduce dependence on chemical pesticides, thereby contributing to more sustainable agricultural systems (Koppenhöfer *et al.* 2020; Nurashikin-Khairuddin *et al.* 2022; van Zyl and Malan 2014). The remarkable pathogenicity of EPNs stems from their symbiotic relationship with specific bacteria. *Steinernema* species exclusively harbor *Xenorhabdus* bacteria, while *Heterorhabditis* species carry *Photorhabdus* bacteria as their symbiotic partners. During host infection, these muturalistic bacteria are released into the insect hemocoel, rapidly inducing host mortality through acute septicemia (San-Blas 2013; Stuart *et al.* 2006).

The EPNs exhibit a near-global distribution, having been reported from all continents except Antarctica. Extensive field surveys have demonstrated their widespread occurrence across diverse ecosystems, particularly in temperate and tropical regions (Bhat *et al.* 2020). The past decade has witnessed significant taxonomic progress in the genus *Steinernema*, with the descriptions of numerous novel species significantly expanding both our understanding of the group's biodiversity and the available options for biological pest control applications (Lacey and Georgis 2012).

The described biodiversity of EPNs currently included 113 validated species in the genus *Steinernema* and 21 species in its sister genus *Heterorhabditis* (Půža *et al.* 2024). The classification of these nematode species employs an integrative taxonomic approach incorporating diagnostic morphological characteristics, species-specific ecological habits, and their relationship with symbiotic bacteria. Molecular phylogenetic analysis based on the sequences of the internal transcribed spacer (ITS) region of ribosomal RNA (rRNA) genes has resolved the species of

the genus *Steinernema* into 12 well-defined clades, comprising nine multispecies clades and three monotypic clades (Spiridonov and Subbotin 2016).

From 2020 to 2024, we conducted a comprehensive survey investigating the occurrence and distribution of EPNs in the Tarim Basin of Xinjiang, China. The survey yielded more than 20 EPN isolates, including three *Steinernema* isolates that were initially identified as conspecificity based on morphological characters, and belonged to the 'kushidai-clade' based on molecular characters (Spiridonov and Subbotin 2016). The 'kushidai-clade' currently comprises four described species including *S. akhursti* Qiu *et al.* 2005, *S. anatnagense* Bhat *et al.* 2023, *S. kushidai* Mamiya, 1988), and *S. populi* Tian *et al.* 2022. Following detailed morphological examinations and phylogenetic analyses, three isolates were confirmed as identical and nominated as *Steinernema tarimense* n. sp. For the taxonomic characterization of this new species, we selected isolate Z32 as the type material, which serves as the basis for both morphological description and biological characterization.

Materials and methods

Nematode isolation and cultivation

During the survey conducted in April 2024, three *Steinernema* isolates (R31, R39, and Z32) were collected from soil of the *Populus euphratica* forest in Yuli County at Tarim Basin of Xinjiang, China. The soil samples were collected from a square of 10 m × 10 m area and taken in a depth of 10–30 cm using a 5-point cross-sampling method. Approximately 500 g homogenized soil from all five sampling points constituted one soil sample. All soil samples were sealed in plastic bags and transported to the laboratory. Seven mature larvae of *Galleria mellonella* were subsequently placed into each bag and mixed thoroughly with the soil. The bags were then kept in the dark at 25°C. After 2–3 days later, the dead *G. mellonella* larvae were collected from soil samples, and the third-stage infective juveniles (IJs) of EPN were recovered from each larva by the White trap method (White 1927). The emerged IJs were collected and cleaned 3–4 times using sterilized water. The IJs suspensions were adjusted to a concentration of approximately 1,000 IJs/ml using a 1% formalin solution, and stored at 10°C in petri dishes (diam. 9 cm). During the preservation period, the IJs were recovered with *G. mellonella* larvae every 3–4 months.

Morphological observations

Different life stages of the isolate Z32 were obtained from the infected *G. mellonella* larvae, which were exposed to 1400 IJs/insects in a 9-cm-diameter Petri dish lined with two moistened filter papers and kept in the dark at 25°C. The first- and second-generation adult nematodes were obtained by dissecting infected *G. mellonella* cadavers in Ringer's solution after 2 and 5 days infection, respectively, under an Olympus SZ61 microscope (Tokyo, Japan). The IJs were collected from the cadavers after 6–8 days infection.

For light microscopy (LM) observation, the above adults and juveniles were killed in 60°C water, fixed in triethanolamine formalin (TAF), and dehydrated using the slow evaporation method (Nguyen 2007a). Dehydration was performed by placing the fixed nematodes in an embryo dish with a 5% glycerin solution and allowing them to slowly evaporate for at least a week. After processed in pure glycerin, the nematodes were subsequently mounted in anhydrous glycerin on permanent slides. The morphological

observations, morphometrics, and photographics were taken under an Olympus CX41 phase contrast microscope. The drawings of morphological characters were performed using a drawing tube connected to an Olympus BHA light microscope, and in conjunction with the Adobe Illustrator CS5.

For scanning electron microscopy (SEM) observation, the first-generation adult males and IJs were fixed in 4% formalin buffered with 0.1 M sodium cacodylate (pH 7.2) for 24 h at 8°C. They were subsequently fixed with a 2% osmium tetroxide solution for 12 h at 25°C, then dehydrated through a graded series of ethanol, critical point dried using liquid carbon dioxide, mounted on SEM stubs, and coated with gold (Nguyen 2007a). Specimens were then photographed using a Regulus 8100 microscope (Hitachi, Tokyo, Japan).

DNA extraction

The DNA of approximate 1,000 IJs from each of three isolates was extracted according to the methods described in Nguyen (2007a). The IJs were collected into a 1.5 ml centrifuge tube and surface-sterilized with 0.1% NaOCl for 30 min. After being centrifuged at 1,000 r/min for 5 min, the nematode precipitate was washed 3 to 5 times with sterile water. After adding proteinase K (final concentration 60 μg/ml), the tube was put in liquid nitrogen for 3 to 5 min and subsequently incubated at 65°C for 5 min. Afterward, the tube was quickly put in liquid nitrogen again for another 3 to 5 min and incubated at 65°C for 5 min. After these steps were repeated 2 to 3 times, the tube was incubated at 95°C for 10 min to degenerate proteinase. Finally, the tube was centrifuged at 12000 r/min for 2 min, and the supernatant was collected as the template for PCR amplification or stored at -20°C.

PCR amplification and sequencing

The near full-length fragment of ITS regions of rRNA genes was amplified from the DNA template with the forward primer 18S (5'-TTG ATT ACG TCC CTG CCC TTT-3') and the reverse primer 26S (5'-TTT CAC TCG CCG TTA CTA AGG-3') (Vrain *et al.* 1992). The fragment of D2-D3 regions of 28S rRNA gene was amplified with the forward primer D2F (5'-CCT TAG TAA CGG CGA GTG AAA-3') and the reverse primer 536 (5'-CAG CTA TCC TGA GGA AAC-3') (Nguyen, 2007a). The fragment of 12S mitochondrial gene (*mt12S*) was amplified with the forward primer 505F (5'-GTT CCA GAA TAA TCG GCT AGA C-3') and the reverse primer 506R (5'-TCT ACT TTA CTA CAA CTT ACT CCC CC-3') (Nadler *et al.* 2006).

The PCR reaction was carried out in a total volume of 25 μl containing 2.5 μl of DNA template, 2.5 μl of 10× PCR buffer, 1 μl of a dNTP mixture (10 mM each), 1 μl of each primer (10 mM), 1.5 μl of MgCl$_2$ (50 mM), and 0.25 μl of Taq DNA polymerase (5 U μl), and adding distilled water to the full volume. The PCR programs for amplifying ITS and 28S fragments were followed by the description in Nguyen (2007a) as: an initial step of 94°C for 7 min; 35 cycles of 94°C for 60 s, 50°C for 60 s, and 72°C for 60 s; a final step of 72°C for 10 min. The PCR program for *mt12S* fragment was as follows: an initial step of 94°C for 3 min; 30 cycles of 94°C for 30 s, 50°C for 30 s, 72°C for 45 s; and a final step of 72°C for 15 min. PCR products were separated on 1% agarose gels and visualised by staining with ethidium bromide. PCR products of sufficiently high quality were purified for cloning and sequencing by the Sangon Bioengineering Co., Ltd. (Shanghai, China).

Phylogenetic analysis

The newly obtained sequences were analyzed using BLAST to identify closely related species and compare them with existing sequences in the GenBank database. The sequences of relevant *Steinernema* species were downloaded from the GenBank. Multiple sequence alignments were generated for these sequences using the default Clustal X 1.8 configuration in software MEGA 7 and were subsequently optimized manually in BioEdit (Hall 1999). Sequences similarities were calculated by Pairwise distances using the MegAlign Pro 17. The sequence datasets were analyzed with the Bayesian inference (BI) on CIPRES Science Gateway v.3.3 (Miller *et al.* 2010) using MrBayes 3.2.3 (Ronquist *et al.* 2012). The best-fitting models were identified based on the Akaike information criterion using the ModelFinder (Kalyaanamoorthy *et al.* 2017). The BI analysis of ITS sequences was performed under the GTR + F + G4 model, while the 28S and *mt12S* sequences were analyzed using the GTR + F + I + G4 model, and the tree topology was confirmed using IQ-TREE (Nguyen *et al.* 2015). Four chains were run for 1×10^7 generations, after which 25% of the sampled trees were discarded as burn-in. The Markov Chain Monte Carlo Algorithms (Larget and Simon 1999) was employed within a Bayesian framework to estimate the posterior probabilities (PP) of phylogenetic trees and to generate a 50% majority-rule consensus tree. Trees were visualized and modified by using the FigTree v. 1.4.3 (Rambaut 2016) and the Adobe Illustrator CS5.

Results

Steinernema tarimense n. sp.

Description

First-generation male

Body slender, ventrally curved posteriorly, strong J-shaped when heat-killed (Figure 1A, Figure 2A). Cuticle annuli appearing slightly visible under SEM (Figure 3A). Lateral fields scarcely marked. Lip region round, continuous with body. Six lips amalgamated, with one acute labial papilla and one low and larger cephalic papilla each, except lateral lips. Amphidial apertures small, located at lateral lips posterior to lateral labial papillae (Figure 3A). Stoma shallow, funnel-shaped, short and wide, with inconspicuous sclerotized walls. Deirids inconspicuous. Pharynx muscular with a cylindrical procorpus, a slightly swollen and non-valvate metacorpus, narrower isthmus and basal bulb spheroid with reduced valves. Nerve ring usually located at anterior part of the basal bulb. Secretory-excretory pore located at level of metacorpus. Cardia prominent, conoid. Intestine tubular without differentiations. Reproductive system monorchic, ventrally reflexed (Figure 1B, Figure 2C). Spicules paired, symmetrical, slightly ventrally curved with manubrium elongated rhomboidal (Figure 1E, Figure 2F), calamus narrower and lamina moderately curved (Figure 2G), slightly arched at anterior part, bearing two longitudinal ribs, and ending in a bluntly pointed terminus, with scarcely developed velum not reaching spicule tip, without rostrum or retinaculum (Figure 2H). Gubernaculum fusiform, with curved and enlarged tip, cuneus pointed, corpus closed posteriorly, about 70% of the length of spicules (Figure 2H). Tail conoid rounded without a fine mucron (Figure 2F, H). Bursa absent. There are 23 genital papillae (GP) (11 pairs and one single) arranged as follows: five pairs subventral precloacal, one pair lateral precloacal, one single midventral papilla precloacal, two pairs sub-ventral ad-cloacal, one pair

subdorsal post-cloacal, and two pairs of subventral terminal papillae. Phasmids terminal, located between GP9 and GP10 pairs (Figure 3B-D).

Second-generation male

General morphology similar to that of first-generation males (Figure 4B, E), but smaller in size and slenderer (Figure 4A). Tail mucron absent. Spicules ventrally curved, with manubrium rounded, calamus slightly narrower than manubrium (Figure 4G), and lamina ventrally curved at anterior part, lanceolate posterior part with finely rounded tip, reduced ventral velum, and two longitudinal lateral ribs. Gubernaculum slenderer than that of first-generation male, with manubrium ventrad bent, corpus robust, and narrow and slender terminus (Figure 4H). Genital papillae and phasmids with arrangement similar to that in first-generation male.

First-generation female

Body C-shaped when heat-relaxed and fixed (Figure 2B). Cuticle with poorly visible annuli. Lateral fields not observed. Deirids inconspicuous, difficult to observe even under SEM. Labial region rounded, continuous with the adjacent part of body (Figure 1C, Figure 2E). Stoma and pharynx region similar to males (Figure 1C). Nerve ring surrounding isthmus, located just anterior to basal bulb. Excretory pore located at level of metacorpus (Figure 2D). Cardia prominent. Reproductive system didelphic, amphidelphic. Ovaries reflexed in dorsal position; oviducts well developed with glandular spermatheca, and uteri tubular with numerous uterine eggs; vagina short, with muscular walls; vulval protruding, in the form of transverse slit located slightly post-equatorial with lips slightly protruding, asymmetrical, without small epiptygmata (Figure 2I). Rectum 0.23 to 0.46 times the body diam., with three rectal glands. Tail conoid, shorter than anal body diam., terminus bearing a minute mucron (Figure 1F, Figure 2J). Phasmids located at anterior part of tail, at 40% to 48% of tail length.

Second-generation female

Similar to first-generation female but smaller. Tail conoid and straight, longer than that of first-generation female (Figure 1G), tapering to a blunt end, lacking mucron (Figure 4J). Excretory pore located at level of metacorpus, similar as that in the first-generation female (Figure 4C). Phasmid located at posterior part of tail, approximately at 60% of tail length

Third-stage infective juvenile

Body slender, straight or slightly curved when heat-killed, tapering gradually from the base of pharynx to the anterior end and from anus to the distal end. Cuticle striated (Figure 5A). appearing well-developed annuli (Figure 5C). Lateral fields begin as a single ridge close to anterior end, increasing to eight ridges unequally spaced, posteriorly gradually reduced to six (anus level) and two (phasmid level) (Figure 5F, G). Lip region truncate, smooth or annulated, continuous or slightly offset from the adjacent part of body, with six lips and prominent six labial and four cephalic papillae (Figure 5B, D). Amphidial apertures rounded and pore-like. Stoma reduced almost closed, with small cheilostom and elongate gymnostegostom. Pharynx reduced with narrow corpus, lightly swollen metacorpus, slightly narrower isthmus, and elongated pyriform basal bulb with reduced valves. Nerve ring surrounding isthmus. Excretory pore located at level of metacorpus. Hemizonid present, located at anterior of pharynx base. Cardia conoid and small. Deirids inconspicuous (Figure 4D, K). Intestine lumen narrow, bearing a bacterial sac at its anterior part (Figure 4L). Rectum long,

almost straight (Figure 1D). Anus distinct (Figure 4M-O, Figure 5H). Genital primordium obscure. Tail conoid, tapering gradually with pointed terminus; hyaline part occupying *ca.* 35.1% of tail length. Phasmids prominent, located at 65% to 75% of tail length (Figure 5E).

Diagnoses and relationships

Steinernema tarimense n. sp. adults have short stoma, pharynx robust with rounded basal bulb; males monorchid with ventrally curved spicules, gubernaculum fusiform in the first and second generations, tail conoid slightly ventrally curved, with blunt terminus; females didelphic-amphidelphic with shorter conoid tail bearing a fine mucron in the first generation (31–74 μm, c = 47.6–120.5, c′ = 0.2–0.4, mucron = 3.7–5.0 μm) and longer conoid tail lacking mucron in the second generation (43–81 μm, c = 31.7–47.5, c′ = 0.4–0.6); and IJs with short body (674–1010 μm), poorly developed pharynx (111–162 μm), H% (25.5–45.1), D% (42.0–66.6), and E% (116–184), lateral fields with eight longitudinal ridges, and tail elongated conoid (41–56 μm, c = 14.7–21.6, c′ = 1.4–1.9) (Table 1).

Steinernema tarimense n. sp. belongs to the 'kushidai-clade' as defined by Spiridonov and Subbotin (2016). Phylogenetic analysis revealed that *S. tarimense* n. sp. is sistered to other members of the 'kushidai-clade', including *S. akhursti*, *S. anatnagense*, *S. kushidai*, and *S. populi*. These species are characterized by the infective juvenile (IJ) body lengths ranging from 700 to 1,000 μm (Bhat *et al.* 2023).

The IJs of *S. tarimense* n. sp. differ from *S. akhursti* in body diameter (24–33 μm vs 33–35 μm), tail length (41–56 μm vs 68-75 μm), a ratio (26.8–32.4 vs 23–26), c ratio (14.7–21.6 vs 10–12), D% value (42.0–66.6 vs 45–50), and E% value (116–184 vs 73–86); from *S. anatnagense* in body diameter (24–33 μm vs 32–42 μm), the distances from anterior end to excretory pore (53–80 μm vs 45–62 μm), to nerve ring (85–131 μm vs 54–71 μm), tail length (41–56 μm vs 49–66 μm), a ratio (26.8–32.4 vs 19–24), c ratio (14.7–21.6 vs 12.2–16.4), D% value (42.0–66.6 vs 35–48), and E% value (116–184 vs 74–113); from *S. kushidai* in body length (674–1010 μm vs 424–662 μm), the distances from anterior end to excretory pore (53–80 μm vs 42–50 μm) and to nerve ring (85–131 μm vs 70–84 μm), ratio a (26.8–32 vs 19–25), ratio c (14.7–21.6 vs 10–13), D% value (42.0–66.6 vs 38–44), and E% value (116–184 vs 92); and from *S. populi* in body diameter (24–33 μm vs 33–41 μm), tail length (41–56 μm vs 55–72 μm), and anal body width (15–20 μm vs 21–27 μm).

The first-generation males of *S. tarimense* n. sp. differ from *S. akhursti* in distances from anterior end to nerve ring (97–136 μm vs 120–163 μm), and to end of pharynx (134–170 μm vs 168–205 μm), spicule length (61–89 μm vs 85–100 μm), and gubernaculum length (41–58 μm vs 58–68 μm); from *S. anatnagense* in body diameter (83–124 μm vs 167–211 μm), anal body width (39–56 μm vs 25–36 μm), ratio a (11.9–17.5 vs 6.4–9.8), spicule length (61–89 μm vs 56–70 μm), gubernaculum length (41–58 μm vs 31–43 μm); from *S. kushidai* in spicule length (61–89 μm vs 48–72 μm); and from *S. populi* in body diameter (83–124 μm vs 66.3–95 μm), tail length (24–42 μm vs 39.2–68 μm), ratio c (33.6–56.0 vs 19.8–32.9), and D% value (36.8–66.2 vs 59–78).

Moreover, the comparison of IJs for species in the 'feltiae-kushidai-clade', which comprises over 20 *Steinernema* species (Table 2) revealed that *S. tarimense* n. sp. can be distinguished from all these species, especially *S. cholashanense* Nguyen, Puza & Mracek, 2008, *S. feltiae* (Filipjev, 1934) Wouts, Mracek, Gerdin & Bedding, 1982, and *S. oregonense* Liu & Berry, 1996 by the smaller body length, longer

distance of excretory pore to anterior end, shorter tail length, as well as the lower ratio b value, higher values in ratio c, D%, and E%. The comparisons of the first-generation males (Table 3) also revealed that the new species differs from *S. cholashanense*, *S. feltiae*, and *S. oregonense* by the longer spicules, lower D% and higher SW% values.

Life cycle

Steinernema tarimense n. sp. demonstrated effective infestation and development in *G. mellonella* larvae (Figure 6), exhibiting significantly faster development rates compared to several congeneric species. At 25°C, *S. tarimense* n. sp. completed its life cycle more rapidly than *S. cholashanense*, *S. feltiae*, *S. litorale*, and *S. populi*. When infected with 100 IJs of *S. tarimense* n. sp., *G. mellonella* larvae succumbed within 2–3 days, compared to 5–6 days for the other species examined. The first- and second-generation adults of *S. tarimense* n. sp. appeared in host cadavers within 2–3 days and 5–6 days post-infection, respectively, while the comparative species required 8–9 days and 11–12 days for the same developmental stages. Notably, the IJs of *S. tarimense* n. sp. emerged from cadavers with 5–6 days after initial infection, whereas the other species showed emergence times of 8–12 days.

Type host and locality

The type hosts are unknown as the nematodes of this genus can be hosted by different insect species (Fallet *et al.* 2022; Kajuga *et al.* 2018; Yan *et al.* 2016). Specimens of *S. tarimense* n. sp. were isolated from mixed soil samples collected in a *Populus euphratica* forest located along the Tarim River (Yuli County, Xinjiang, China) using the *Galleria mellonella* baiting technique (Bedding and Akhurst 1975; White 1927). The geographic coordinates of the sampling site for isolate R31 is 41°3′44.3592″N and 86°7′2.0279″E, for isolate R39 is 41°4′20.37″N and 86°7′9.6312″E, and for isolate Z32 is 41° 4′25.0824″N and 86°7′3.3708″E.

Type material

Isolate Z32 was designated as the type material for *Steinernema tarimense* n. sp. Three slides of each stage, including first-generation adults (males and females), second-generation adults (males and females), and IJs, were deposited in the US Department of Agriculture Nematode Collection (USDA NC), Beltsville, Maryland, USA. Holotype: one male of F1, USDANC accession numbers is T-811t. Paratype: males of F1, with USDANC numbers from T-8097p to T-8099p; males of F2, with numbers from T-8103p to T-8105p; females of F1, with numbers from T-8106p to T-8108p; females of F2, with numbers from T-8109p to T-8110p; IJs, with numbers from T-8100p to T-8013p.

Many males and females of the first generation and several IJs were deposited in the National Parasitic Resources Center (NPRC-2019-194-30) of China, with accession No. CSTR:15507.06. YZ1CR1001KpLC.

Numerous males and females of the first generation, along with several IJs, were deposited in the Institute of Microbiology, Xinjiang Academy of Agricultural Sciences, China.

Etymology

The species epithet refers to the region where the species was recovered (Tarim Basin in Xinjiang, China).

Nematode molecular characterization

The ITS sequences of *Steinernema tarimense* n. sp. isolates R31, R39, and Z32 were identical in length of 1019 bp, with GenBank accession number PQ590687, PQ590686, and PQ590685, respectively (Table 4) . The sequence similarity of three isolates is 100%. Comparative sequence analysis revealed that the ITS region of *S. tarimense* n. sp. exhibited 76–124 nucleotide differences relative to related species, corresponding to sequence similarity values ranging from 84.50% to 92.09% (Supplementary table 1). The

sequence similarity of the new species to *S. anantnagense* (OQ407501) is 92.09%; to *S. akhursti* (DQ375757), 91.40%; to *S. kushidai* (AB243440), 90.17%; to *S. cholashanense* (EF431959), 84.99%; and to *S. populi* (MZ367622), 84.50%.

The 28S sequences of isolates R31, R39, and Z32 were identical in length of 908 bp, with GenBank No. PQ590690, PQ590689, and PQ590688, respectively (Table 4). Three sequences of the new species showed 100% similarity, while exhibiting 8–20 nucleotide differences from related species, corresponding to sequence

Table 1. Morphometrics of *Steinernema tarimensis* n. sp. All measurements are in μm and in the form: mean ± s.d. (range)

| Character | First generation | | | Second generation | | |
| | Male | Female | Male | Female | Infective juvenile |
	Holotype	Paratypes	Paratypes	Paratypes	Paratypes	Paratypes
n	—	25	25	25	25	25
Body length (L)	1505	1448 ± 174 (1199–1838)	4522 ± 1726 (2600–7712)	1355 ± 109 (1168–1550)	2675±340.9 (1914–3292)	790 ± 98 (674–1010)
a (L/BD)	16.6	13.7±1.5 (11.9–17.5)	19.2 ± 2.3 (15.8–25.0)	15.4 ± 1.4 (13.6–18.8)	20.5 ± 1.8 (16.3–23.4)	29.3 ± 1.6 (26.8–32.4)
b (L/NL)	8.9	9.3 ± 1.1 (7.7–11.9))	21.2 ± 5.3 (13.6–31.0)	8.4 ± 0.7 (7.0–9.9)	12.1 ± 1.4 (8.8–14.7)	5.9 ± 0.7 (5.0–7.6)
c (L/T)	43.9	42.2 ± 7.4 (33.6–56.0)	80.0 ± 19.8 (47.6–120.5)	39.3 ± 5.1 (29.9–47.8)	40.4 ± 4.2 (31.7–47.5)	17.0 ± 1.8 (14.7–21.6)
c' (T/ABD)	0.4	0.3 ± 0.1 (0.3–0.4)	0.3 ± 0.1 (0.2–0.4)	0.4 ± 0.1 (0.3–0.6)	0.5 ± 0.1 (0.4–0.6)	1.7 ± 0.2 (1.4–1.9)
Max. body diam. (BD)	90.9	105 ± 9.0 (83–124)	239 ± 95.6 (126–416)	88 ± 7.6 (71–103)	131 ± 14.0 (104–165)	27 ± 2.6 (24–33)
Excretory pore to anterior end (EP)	65.1	81 ± 10.5 (62–105)	94 ± 21.4 (45–128)	76 ± 14.2 (55–98)	113 ± 8.5 (95–130)	70 ± 6.2 (53–80)
Nerve ring to anterior end (NR)	131	119 ± 8.8 (97–136)	154 ± 21.3 (106–191)	122 ± 7.1 (107–130)	160 ± 9.0 (131–175)	112 ± 12.3 (85–131)
Neck length (stoma+pharynx, NL)	168	156 ± 8.9 (134–170)	208 ± 30.9 (143–252)	161 ± 12.0 (130–179)	222 ± 10.1 (195–240)	134 ± 13.8 (111–162)
Testis reflexion	533	413 ± 79.3 (312–633)	—	371 ± 31.6 (321–425)	—	—
Tail length (T)	34.2	35 ± 4.8 (24–42)	56 ± 11.7 (31–74)	34 ± 4.0 (27–42)	66 ± 7.1 (43–81)	46 ± 3.7 (41–56)
Anal body diam. (ABD)	43.3	49±4.2 (39–56)	74 ± 23.5 (43–124)	44 ± 3.3 (40–52)	42 ± 4.5 (35–52)	16 ± 1.1 (15–20)
Spicule length (SL)	72.0	76±6.4 (61–89)	—	72 ± 6.2 (58–85)	—	—
Gubernaculums length (GL)	50.3	48 ± 4.1 (41–58)	—	41 ± 4.2 (33–47)	—	—
Hyaline tail length (HT)	—	—		—	—	16 ± 2.6 (12–21)
D% (EP/NL×100)	38.7	52.0 ± 7.3 (36.8–66.2)	45.7 ± 8.7 (21.7–58.6)	47.9 ± 9.7 (32.6–67.8)	51.2 ± 4.1 (42.1–60.6)	52.6 ± 6.3 (42.0–66.6)
E% (EP/T×100)	190	237 ± 44.5 (187–340)	173 ± 34.9 (77.9–223)	222 ± 41.4 (139–291)	172 ± 16.3 (142–231)	152 ± 18.1 (116–184)
SW% (SL/ABD×100)	166	157 ± 22.6 (117–206)	—	166 ± 14.4 (132–190)	—	—
GS% (GL/SL×100)	69.9	63.5 ± 7.2 (54.8–82.0)	—	57.6 ± 5.2 (46.5–67.4)	—	—
H% (HT/T×100)	—	—	—	—	—	35.1 ± 5.7 (25.5–45.1)

Table 2. Comparison of morphometrics of infective juveniles of *Steinernema tarimense* n. sp. with other members of '*feltiae-kushidai*-clade'. Measurements are in µm except n, ratio and percentage. Data for new species is in bold

Species	n	L	BD	EP	NR	NL	T	ABD	a	b	c	D%	E%	Reference
S. tarimense n. sp.	**25**	**790 (674–1010)**	**27 (24–33)**	**70 (53–80)**	**112 (85–131)**	**134 (111–162)**	**46 (41–56)**	**16 (15–20)**	**29.3 (26.8–32.4)**	**5.9 (5.0–7.6)**	**17.0 (14.7–21.6)**	**52.6 (42.0–66.6)**	**152 (116–184)**	**Present study**
S. akhursti	20	812 (770–835)	33 (33–35)	59 (55–60)	90 (83–95)	119 (115–123)	73 (68–75)	20 (19–20)	24 (23–26)	6.8 (6.6–7.2)	11 (10–12)	47 (45–50)	77 (73–86)	Qiu *et al.* (2005)
S. anatnagense	20	789 (749–834)	37 (32–42)	55 (45–62)	63 (54–71)	132 (120–143)	58 (49–66)	20 (18–22)	22 (19–24)	6 (5.5–6.7)	13.8 (12.2–16.4)	42 (35–48)	96 (74–113)	Bhat *et al.* (2023)
S. cholashanense	20	843 (727–909)	30 (26–35)	62 (59–65)	87 (72–97)	125 (110–138)	73 (60–80)	17 (16–19)	28 (24–34)	6.8 (6.1–7.2)	12 (10–14)	49 (46–53)	81 (76–91)	Nguyen *et al.* (2008)
S. citrae	20	754 (623–849)	26 (23–28)	56 (49–64)	98 (83–108)	125 (118–137)	71 (63–81)	14 (13–17)	30 (25–34)	6.0 (5.1–7.1)	15 (13–14)	44 (39–58)	110 (85–132)	Stokwe *et al.* (2011)
S. feltiae	25	849 (766–928)	29 (22–32)	63 (58–67)	113 (108–117)	136 (130–143)	86 (81–89)	18 (16–19)	30 (27–34)	6.4 (5.8–6.8)	10 (9.4–11)	46 (44–50)	74 (67–81)	Nguyen (2007b)
S. hebeiense	20	658 (610–710)	26 (23–28)	48 (43–51)	78 (73–83)	107 (100–111)	66 (63–71)	NA	26 (24–28)	6.2 (5.7–6.7)	10 (9.4–11)	45 (40–50)	72 (65–80)	Chen *et al.* (2006)
S. ichnusae	20	866 (767–969)	32 (27–35)	63 (59–68)	102 (94–108)	138 (119–148)	81 (76–89)	18 (17–19)	28 (24–32)	6.3 (5.6–6.9)	11 (8.8–12)	46 (42–49)	77 (68–83)	Tarasco *et al.* (2008)
S. jollieti	25	711 (625–820)	23 (20–28)	60 (53–65)	NA	123 (115–135)	68 (60–73)	15 (13–18)	31 (25–34)	5.7 (4.9–6.4)	10.5 (9.0–11.7)	48 (46–50)	88	Spiridonov *et al.* (2004)
S. kraussei	25	951 (797–1102)	33 (30–36)	63 (50–66)	105 (99–111)	134 (119–145)	79 (63–86)	20 (19–22)	29	7.1	12.1	47	80	Nguyen (2007b)
S. kushidai	20	589 (424–662)	26 (22–31)	46 (42–50)	76 (70–84)	111 (106–120)	50 (44–59)	NA	22.5 (19–25)	5.3 (4.9–5.9)	11.7 (10–13)	41 (38–44)	92	Mamiya (1988)
S. litorale	25	909 (834–988)	31 (28–33)	61 (54–69)	96 (89–104)	125 (114–133)	83 (72–91)	19 (16–22)	29.5 (27–31)	7.3 (6.7–7.9)	11 (9.7–11.9)	49 (44–56)	73 (68–84)	Yoshida (2004)
S. nguyeni	20	737 (673–796)	25 (22–28)	52 (47–58)	80 (74–86)	110 (101–121)	67 (61–73)	15 (13–17)	29 (27–33)	6.7 (6.2–7.4)	11 (10–12)	48 (43–57)	79 (70–86)	Malan *et al.* (2016)
S. oregonense	20	980 (820–1110)	34 (28–38)	66 (60–72)	NA	132 (116–148)	70 (64–78)	14 (13–16)	30 (24–37)	7.6 (6–8)	14 (12–16)	50 (40–60)	100 (90–110)	Liu & Berry (1996)
S. populi	25	1095 (973–1172)	36 (33–41)	77 (70–86)	106 (98–113)	149 (134–159)	64 (55–72)	23 (21–27)	30 (24–33)	7.4 (6.8–8.5)	17 (15–20)	52 (47–61)	121 (105–140)	Tian *et al.* (2022)
S. puntauvense	19	670 (631–728)	33 (31–38)	25 (20–30)	54 (46–69)	94 (81–103)	54 (51–59)	17 (15–18)	20 (17–23)	6.1 (7.1–7.9)	12 (11–13)	42 (25–50)	44 (35–56)	Uribe–Lório *et al.* (2007)
S. sandneri	25	843 (708–965)	27 (23–32)	56 (44–64)	103 (83–118)	138 (123–151)	75 (64–86)	19 (15–24)	29 (23–33)	6.1 (5.5–6.9)	11.2 (11–13.2)	40 (36–45)	74 (63–86)	Lis *et al.* (2021)
S. sangi	20	753 (704–784)	35 (30–40)	52 (46–54)	91 (78–97)	127 (120–138)	81 (76–89)	18 (17–19)	22 (19–25)	5.9 (5.6–6.3)	9.3 (8.7–10.2)	40 (36–44)	62 (56–70)	Phan *et al.* (2001)
S. silvaticum	21	860 (670–975)	30 (26–35)	62 (51–73)	96 (75–109)	121 (100–141)	75 (63–86)	17 (15–24)	31 (27–34)	7.1 (6.3–7.7)	11.4 (9.9–13.1)	50 (46–56)	83	Sturhan *et al.* (2005)

(Continued)

Table 2. (*Continued*)

Species	n	L	BD	EP	NR	NL	T	ABD	a	b	c	D%	E%	Reference
S. texanum	20	756 (732–796)	30 (29–34)	59 (52–62)	92 (84–102)	115 (111–120)	73 (60–79)	18 (17–20)	25 (22–27)	6.5 (6.2–7.0)	10 (9.6–12.5)	51 (46–53)	81 (76–88)	Nguyen *et al.* (2007)
S. tielingense	20	915 (824–979)	35 (32–38)	69 (64–73)	98 (90–105)	128 (120–135)	81 (74–85)	21 (19–23)	26 (23–28)	7 (6–8)	11 (9–13)	55 (47–61)	88 (85–94)	Ma *et al.* (2012a)
S. weiseri	20	740 (586–828)	25 (24–29)	57 (43–65)	84 (72–92)	113 (95–119)	60 (49–68)	17 (14–19)	29 (25–33)	6.6 (5.7–7.2)	12 (10–14)	51 (44–55)	95	Mrácek *et al.* (2003)
S. xinbinense	20	694 (635–744)	30 (28–31)	51 (46–53)	86 (75–90)	116 (109–125)	73 (65–78)	17 (16–19)	24 (21–25)	6.1 (5–7)	9.7 (8–11)	44 (40–47)	71 (65–78)	Ma *et al.* (2012b)
S. xueshanense	20	860 (768–929)	30 (29–33)	67 (60–72)	91 (81–96)	135 (130–143)	87 (80–92)	19 (17–21)	28 (26–32)	6.4 (5.8–7.0)	9.9 (9.0–11)	50 (46–52)	78 (70–90)	Mrácek *et al.* (2009)

Table 3. Comparison of morphometrics of the first-generation males of *Steinernema tarimense* n. sp. with other members of 'feltiae-kushidai-clade'. Measurements are in μm except n, ratio and percentage. Data for new species is in bold

Species	n	L	BD	EP	NR	NL	T	ABD	SL	GL	a	b	c	D%	SW%	GS%	Mucron
S. tarimense n. sp.	**25**	**1448 (1199–1838)**	**105 (83–124)**	**81 (62–105)**	**119 (97–136)**	**156 (134–170)**	**35 (24–42)**	**49 (39–56)**	**76 (61–89)**	**48 (41–58)**	**13.7 (11.9–17.5)**	**9.3 (7.7–11.9)**	**42.2 (33.6–56.0)**	**52.0 (36.8–66.2)**	**156 (117–206)**	**63.5 (54.8–82.0)**	**P**
S. akhursti	20	1589 (1350–1925)	131 (115–150)	102 (93–113)	136 (120–163)	182 (168–205)	35 (30–40)	51 (45–70)	90 (85–100)	64 (58–68)	NA	NA	NA	56 (52–61)	180 (140–200)	71 (65–77)	P
S. anatnagense	20	1618 (1223–1899)	194 (167–211)	111 (88–124)	112 (103–129)	176 (165–185)	34 (29–39)	32 (25–36)	64 (56–70)	36 (31–43)	8.3 (6.4–9.8)	9.2 (7.0–11.3)	49 (34–64)	63 (49–74)	208 (154–297)	57 (46–70)	P
S. cholashanense	20	1428 (1070–1778)	137 (73–204)	99 (75–135)	106 (91–126)	152 (135–173)	35 (29–43)	49 (38–60)	66 (60–71)	39 (32–45)	11 (7.8–24)	9.3 (7.5–11.2)	41 (36–51)	64 (50–85)	115 (92–144)	71 (61–85)	P
S. citrae	20	1154 (1028–1402)	103 (87–113)	81 (64–92)	106 (92–119)	139 (123–155)	25 (17–31)	33 (28–43)	65 (57–80)	44 (32–59)	NA	NA	NA	58 (47–67)	198 (156–233)	68 (48–89)	P
S. feltiae	25	1612 (1414–1817)	140 (121–162)	115 (110–126)	NA	170 (164–180)	39 (37–43)	48 (43–53)	70 (65–77)	41 (34–47)	11.5	9.5	41.3	60 (51–64)	113 (99–130)	59 (52–61)	p
S. hebeiense	20	1177 (1036–1450)	86 (74–98)	64 (58–73)	84 (78–93)	126 (118–132)	30 (24–35)	41 (36–53)	57 (51–63)	46 (38–50)	14 (12–17)	9 (8–11)	39 (30–49)	51 (48–59)	140 (120–170)	80 (60–90)	A
S. ichnusae	20	1341 (1151–1494)	137 (73–204)	101 (94–108)	NA	165 (135–173)	40 (33–48)	48 (41–56)	66 (64–67)	44 (43–46)	22 (20–29)	8.2 (7.0–9.4)	34 (29–39)	62 (59–65)	139 (120–162)	67 (64–69)	A
S. jollieti	20	1662 (1296–1952)	1153 (98–135)	98 (83–110)	NA	156 (110–168)	33 (24–38)	44 (40–50)	64 (55–70)	54 (45–60)	15 (12–19)	11 (8.1–14)	51 (53–86)	64 (53–83)	145	84	A
S. kraussei	20	1400 (1200–1600)	128 (110–144)	81 (73–99)	105 (95–122)	153 (137–178)	39 (36–44)	45 (39–50)	49 (42–53)	33 (29–37)	11	9	37	53	110	67	P
S. kushidai	20	1400 (1200–1900)	97 (75–156)	84 (71–105)	129 (120–137)	167 (156–189)	33 (30–40)	42 (36–54)	63 (48–72)	44 (39–60)	NA	NA	NA	51 (42–59)	150	70	A
S. litorale	25	1360 (1230–1514)	96 (82–111)	96 (77–107)	114 (94–128)	147 (133–163)	34 (26–41)	43 (37–49)	75 (67–89)	53 (44–64)	14 (12–16)	9.3 (8.3–10)	41 (33–56)	40 (34–56)	174 (154–200)	71 (62–81)	P
S. nguyeni	20	997 (818–1171)	82 (58–106)	59 (47–71)	91 (70–103)	124 (112–144)	21 (18–25)	31 (27–34)	66 (58–75)	43 (30–55)	12 (11–15)	8.0 (7.0–9.5)	46 (38–53)	48 (38–57)	215 (185–279)	66 (46–81)	P
S. oregonense	20	1680 (1560–1820)	138 (105–161)	120.7 (95–139)	111 (101–133)	154 (139–182)	29 (24–32)	47 (38–55)	71 (65–73)	56 (52–59)	NA	NA	NA	73 (64–75)	151	79	A
S. populi	25	1378 (1258–1514)	82.3 (66.3–95)	107 (94.9–121)	126.9 (107–143)	156 (131–177)	50.9 (39.2–68)	41 (41–60)	66 (57–77)	46 (38–60)	16.9 (14.8–20)	8.9 (7.7–10.1)	27.3 (19.8–32.9)	69 (59–78)	129 (107–160)	70 (58–82)	P/A
S. puntauvense	19	1591	119 (101–139)	94 (68–114)	115 (104–128)	140 (130–158)	33 (28–40)	46 (40–55)	77 (71–81)	34 (30–40)	NA	NA	NA	67 (45–85)	170 (140–200)	65 (55–75)	P
S. sandneri	25	1461 (1205–1635)	155 (123–177)	80.4 (63–92.4)	126 (112–138)	157 (147–169)	41 (35.4–45.5)	54 (50–59.2)	60 (53–65)	44 (39–50)	9.5 (8.5–11.0)	9.3 (8.0–10.2)	35.6 (31–41.9)	51 (42–59)	111 (97–127)	79 (61–83)	P
S. sangi	20	1774 (1440–2325)	159 (120–225)	82 (67–99)	126 (109–166)	166 (150–221)	32 (27–42)	43 (40–50)	63 (58–80)	40 (34–46)	NA	NA	NA	49 (42–63)	150 (120–160)	60 (50–70)	P

(Continued)

Table 3. (*Continued*)

Species	n	L	BD	EP	NR	NL	T	ABD	SL	GL	a	b	c	D%	SW%	GS%	Mucron
S. texanum	20	1296 (1197–1406)	99 (81–116)	90 (79–100)	104 (94–114)	135 (123–147)	23 (19–30)	38 (31–45)	60 (55–66)	45 (39–53)	NA	NA	NA	67 (58–73)	157 (127–203)	75 (62–84)	A
S. tielingense	20	1778 (1430–2064)	129 (111–159)	114 (94–133)	112 (96–132)	160 (145–173)	26 (22–33)	47 (40–52)	88 (79–98)	62 (49–70)	14 (11–18)	11 (9–13)	70 (57–85)	71 (64–78)	191 (176–212)	73 (59–82)	A
S. weiseri	20	1180 (990–1395)	112 (84–138)	70 (57–84)	99 (94–115)	141 (134–154)	25 (19–32)	38 (29–43)	68 (62–72)	53 (46–57)	11 (9.0–12)	8.0 (7.0–10)	48 (36–64)	49 (39–60)	180 (150–240)	80 (70–85)	A
S. xinbinense	20	1265 (1133–1440)	103 (90–126)	68 (57–75)	106 (91–120)	149 (138–159)	37 (30–41)	41 (36–46)	56 (49–62)	35 (30–41)	12 (11–13)	8.5 (7–9)	34 (31–39)	45 (41–50)	137 (114–156)	63 (54–72)	P
S. xueshanense	20	1589 (1313–2040)	144 (97–159)	128 (113–137)	NA	160 (151–175)	38 (29–48)	50 (37–67)	76 (66–91)	49 (41–60)	12 (10–14)	10 (8.0–12)	42 (33–48)	80 (73–87)	152 (93–172)	64 (58–95)	A

Note: NA = Not available; P = Present; A = Absent.

Table 4. Molecular information for nematode species used in phylogenetic analyses. Data of the new species are shown in bold

Nematode species	Isolate code	Geographic origin	GenBank accession number		
			ITS	28S	12S
S. tarimense n. sp.	**R31**	**China**	**PQ590687**	**PQ590690**	**PQ590693**
S. tarimense n. sp.	**R39**	**China**	**PQ590686**	**PQ590689**	**PQ590692**
S. tarimense n. sp.	**Z32**	**China**	**PQ590685**	**PQ590688**	**PQ590691**
S. abbasi	S–01	India	AY248749	–	–
S. africanum	RW14–M–C2a–3	Rwanda	ON041032	OM415988	–
S. akhursti	YNb112	China	DQ375757	AY177188	OQ401048
S. anantnagense	Steiner_8	India	OQ407501	OQ407489	–
S. apuliae	CS3	Italy	–	GU569044	GU569025
S. arenarium	Voronezh	Russia	DQ314288	AF331892	AY944005
S. ashiuense	Type	Japan	–	FJ165550	–
S. bicornutum	Type	Yugoslavia	AF121048	–	–
S. boemarei	Grand Travers	France	–	GU569046	GU569027
S. braziliense	Porto Murtinho	Brazil	–	FJ410326	–
S. ceratophorum	Type l	China	AY230165	–	–
S. cholashanense	Tibet	China	EF431959	EF520284	OQ401049
S. cubanum	Pinar del Rio	Cuba	AY230166	–	AY944009
S. diaprepesi	FL	USA	AF122021	GU569048	AY944010
S. feltiae	Malka	Jordan	EU200355	–	AY944011
S. feltiae	Bodega Bay	USA	–	AF331906	–
S. glaseri	NC	USA	GU395635	AF331908	AP017466
S. guangdongense	GDc339	China	AY170341	–	–
S. hermaphroditum	T87	Indonesia	JQ687355	–	AY944013
S. ichnusae	Sardinia	Italy	–	–	OM422700
S. indicum	NBAIRS58	India	OQ341465	–	–
S. jollieti	Monsanto	USA	–	GU569051	–
S. karii	Type	Kenya	AY230173	–	
S. karii	N20	Kenya	–	–	*AY944015*
S. khoisanae	SF80	South Africa	–	–	GU569033
S. kraussei	Westphalia	Germany	AY230175	AF331896	–
S. kushidai	Hamakita	Japan	AB243440	AF331897	AY944017
S. litorale	IbKt142	Japan	–	–	AP017468
S. longicaudum	CF1 VII	USA	–	–	GU569035
S. monticolum	Type	USA	AF122017	EF439651	AY944020
S. oregonense	Oregon	USA	AF122019	AF331891	–
S. phyllophagae	Type strain	USA	FJ410327	FJ666054	–
S. populi	Jan–72	China	MZ367621	MZ367685	–
S. puertoricense	Loiza	Puerto Rico	–	AF331903	AY944022
S. puntauvense	Li 6	Costa Rica	–	EF187018	GU569037
S. ramanai	IISR–EPN 03	India	KP688395	–	–
S. sacchari	SB10	South Africa	KC633095	–	–
S. sangi	Type	Vietnam	–	–	GU569038

<div align="right">(Continued)</div>

Table 4. (*Continued*)

Nematode species	Isolate code	Geographic origin	GenBank accession number		
			ITS	28S	12S
S. shori	NBAIRS80	India	OR194554	–	–
S. siamkayai	T9	Thailand	AF331917	–	–
S. texanum	Texas	USA	–	EF152569	–
S. vulcanicum	ESC1	Italy	GU929442	–	GU929443
S. weiseri	Type	Turkey	–	GU569059	GU569040
S. xinbinense	LFS48	China	–	GU994204	–
S. xueshanense	Yunnan	China	–	FJ666053	OQ401050

Note: "–" indicates data unavailable.
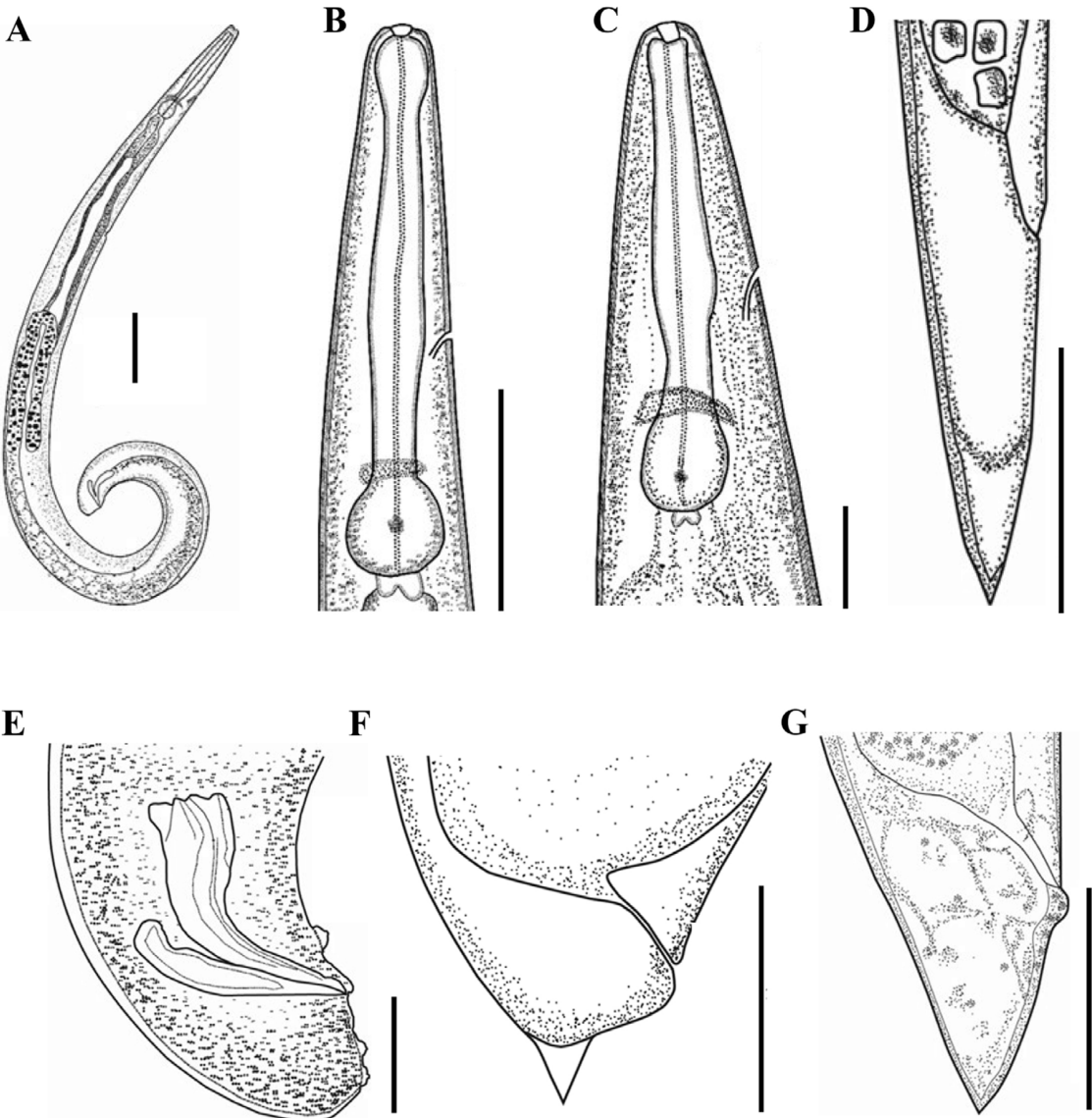
Figure 1. Line drawings of *Steinernema tarimense* n. sp. A: Entire body of first-generation male; B: Stoma and pharynx region of first-generation male; C: Stoma and pharynx region of first-generation female; D: Posterior end of third-stage infective juvenile; E: Posterior end of second-generation male; F: Posterior end of first-generation female with tail mucron; G: Posterior end of second-generation female. Scale bars: A = 100 μm; B, C, E-G = 50 μm; D = 25 μm.
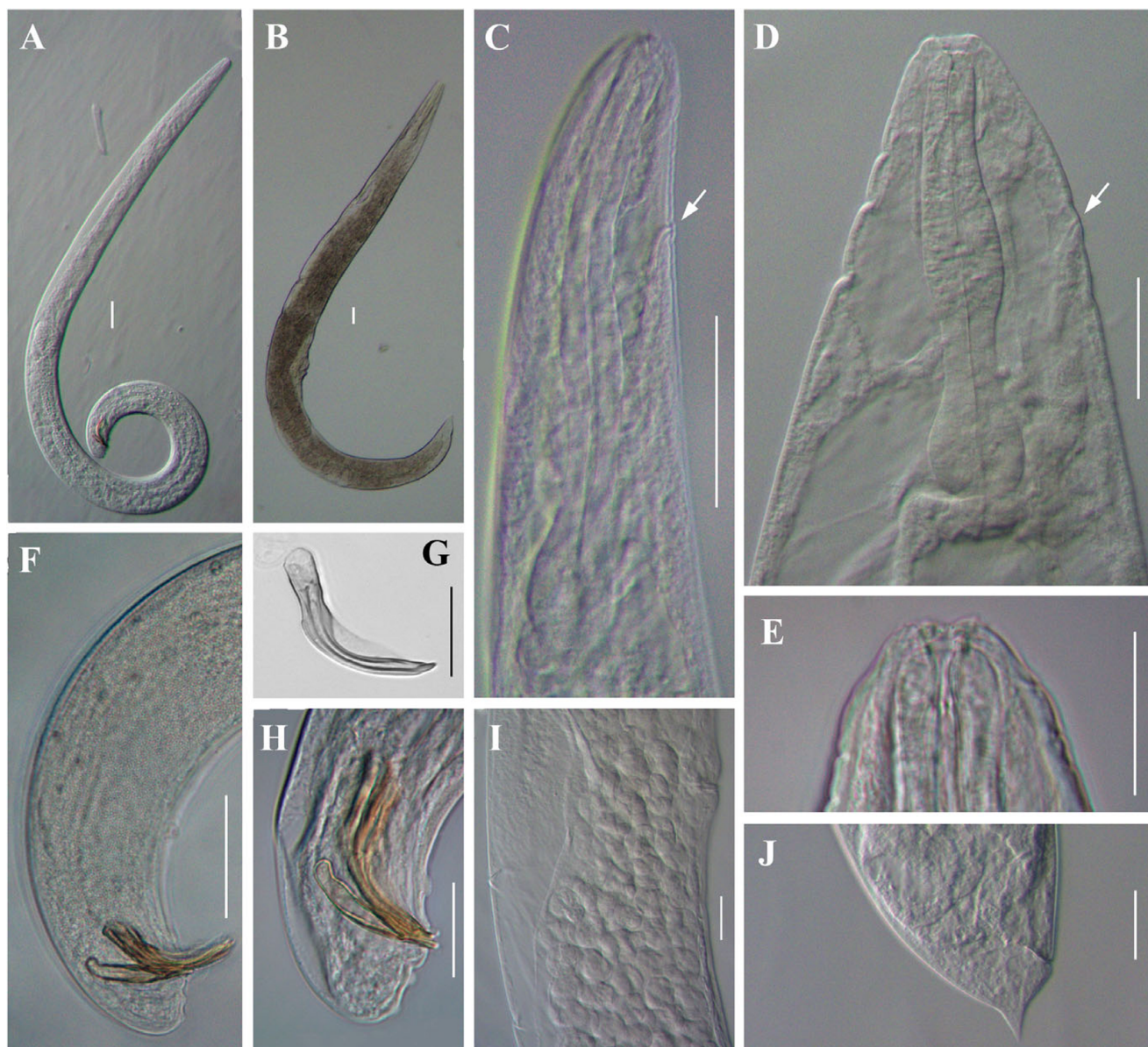
Figure 2. Light microscope micrographs of first-generation adults of *Steinernema tarimensis* n. sp. A, B: Entire body of male and female, respectively; C, D: Stoma and pharynx region of male and female, respectively; E: Lip region and stoma of female; F, H: Posterior end of male; G: Male spicule; I: Vulval region of female; J: Posterior end of female. White arrow pointing the excretory pore. Scale bars: A–D, F, I, J = 50 μm; E, G, H = 25 μm.

similarities of 97.74–98.70% (Supplementary table 2). The sequence similarity of the new species to *S. akhursti* (DQ375757) is 98.47%; to *S. kushidai* (AB243440), 97.91%; and to *S. populi* (MZ367622), 97.74%.

The sequences of *mt12S* gene of isolates R31, R39, and Z32 were identical in length of 546 bp, with GenBank No. PQ590693, PQ590692, and PQ590691, respectively (Table 4). The three sequences of the new species were identical to each other but exhibited significant divergence from related species, with 33–46 nucleotide differences corresponding to sequence similarities of 90.02–91.49% (Supplementary table 3). The sequence similarity of the new species to *S. akhursti* (OQ401048) is 91.49%; to *S. vulcanicum* (GU929443), 91.27%; and to *S. kushidai* (AY944017), 90.02%.

Although *S. tarimense* n. sp. shared relatively low similarity in the ITS, 28S, and *mt12S* sequences with all other known *Steinernema* species, the comparative sequences analysis revealed that the new species is most similar to *S. akhursti*, *S. anantnagense*, and *S. kushidai*, supporting its designation as a novel taxonomic entity within the 'kushidai-clade'.

Nematode phylogenetic relationships

For the ITS sequences, the Bayesian inference (BI) analysis revealed the alignment comprising 1335 nucleotide sites, including 364 constant, 735 parsimony-informative, and 248 singleton sites. The phylogenetic relationships among 27 *Steinernema* species are shown in Figure 7. Three *S. tarimense* n. sp. isolates grouped
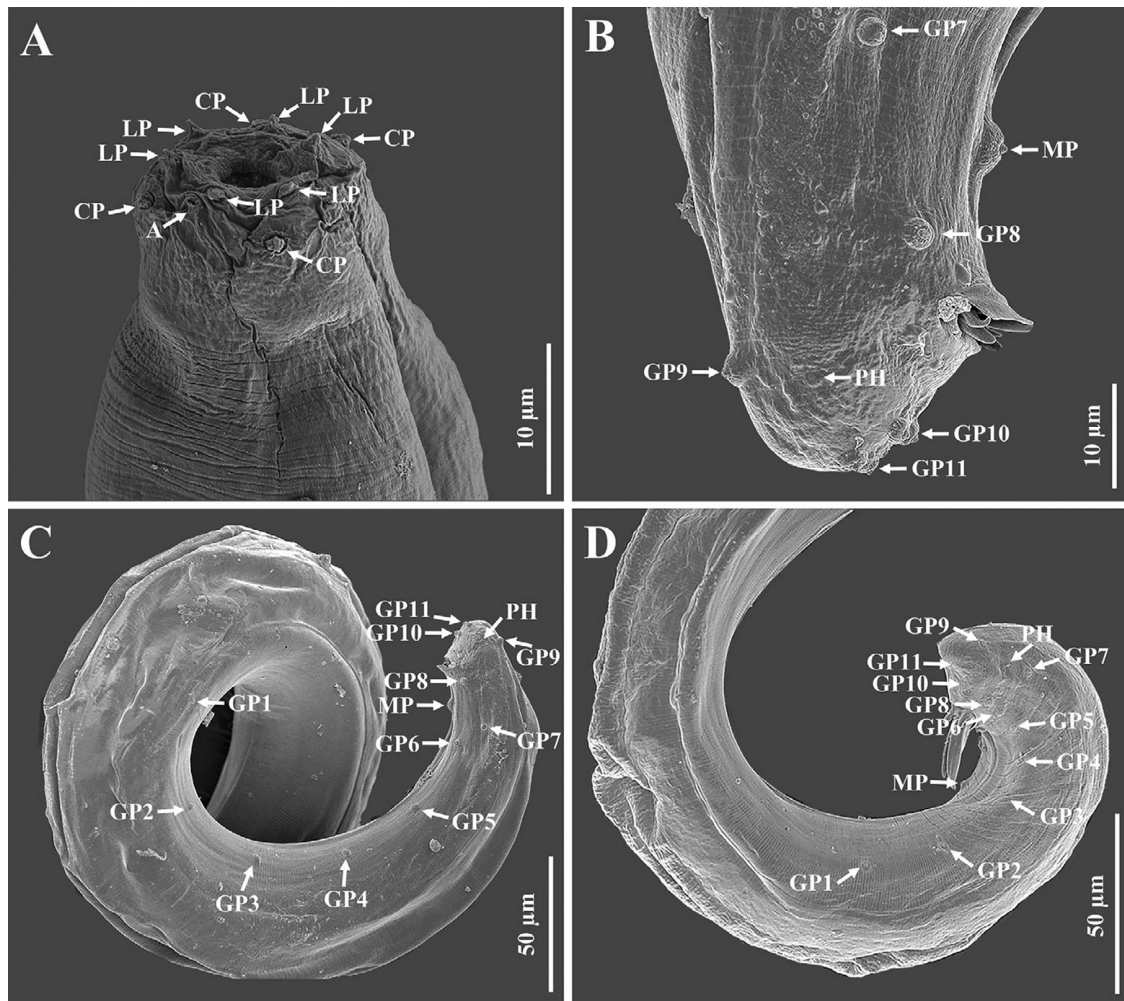
Figure 3. Scanning electron microscope micrographs of the first-generation male of *Steinernema tarimense* n. sp. A: Lip region shown in both dorsal and lateral views; B: Tail region; C, D: Posterior part of body. (Abbreviations: A = amphid; CP = cephalic papilla; LP = labial papilla; MP = mid-ventral papilla; PH = phasmid; GP + number = genital papillae)

with *S. populi* in one branch, which further grouped with the branch consisting of *S. akhursti*, *S. anantnagense* and *S. kushidai* and the branch of '*feltiae*-clade' species including *S. africanum*, *S. chola-shanense*, *S. feltiae*, *S. kraussei*, and *S. oregonense*, into a higher statistically supported '*feltiae-kushidai*-clade' (PP = 96).

For the 28S sequences, the BI analysis revealed the alignment comprising 1030 nucleotide sites, including 583 constant, 267 parsimony-informative, and 180 singleton sites. The phylogenetic relationships among 26 *Steinernema* species are illustrated in Figure 8. Three *S. tarimense* n. sp. isolates grouped with the '*kushidai*-clade' members including *S. akhursti*, *S. anantnagense*, *S. kushidai*, and *S. populi* in a lower supported clade (PP < 50). This clade is further grouped with the members of the '*feltiae*-clade' and '*monticolum*-clade' into a superclade with a highest support (PP = 100).

For the *mt12S* sequences, the BI analysis revealed the alignment encompassing 558 nucleotide sites, including 278 constant, 211 parsimony-informative, and 69 singleton sites. The phylogenetic relationships among 24 *Steinernema* species are illustrated in Figure 9. Three *S. tarimense* n. sp. isolates also grouped with the '*kushidai*-clade' members *S. akhursti* and *S. kushidai* in a lower supported clade (PP < 50). All phylogenetic analyses based on ITS,

28S, and *mt12S* sequences demonstrated that three isolates of *S. tarimense* n. sp. are conspecific and closed to members in the '*kushidai*-clade'.

Discussion

Entomopathogenic nematodes (EPNs) have obtained increasing attention as effective biopesticides for insect pest control. While the diversity of EPNs in China remains incompletely characterized, at least eighteen steinernematids have been originally described from various regions, including Hebei, Jilin, and Yunnan provinces (Chen *et al.* 2006; Ma *et al.* 2012 a, b; Qiu *et al.* 2005; Tian *et al.* 2022). A survey conducted in Xinjiang during 2020 to 2024 has recovered more than 20 EPN isolates, among which three morphologically and genetically identical isolates were identified as a new species – *Steinernema tarimense* n. sp. This species was collected from *Populus euphratica* riparian forests in the Tarim Basin, though its natural insect host remains undetermined. Notably, Xinjiang covers approximately 1.6 million km^2 (one-sixth of China's total territory), making this discovery particularly significant. As the first EPN species described from this vast region,
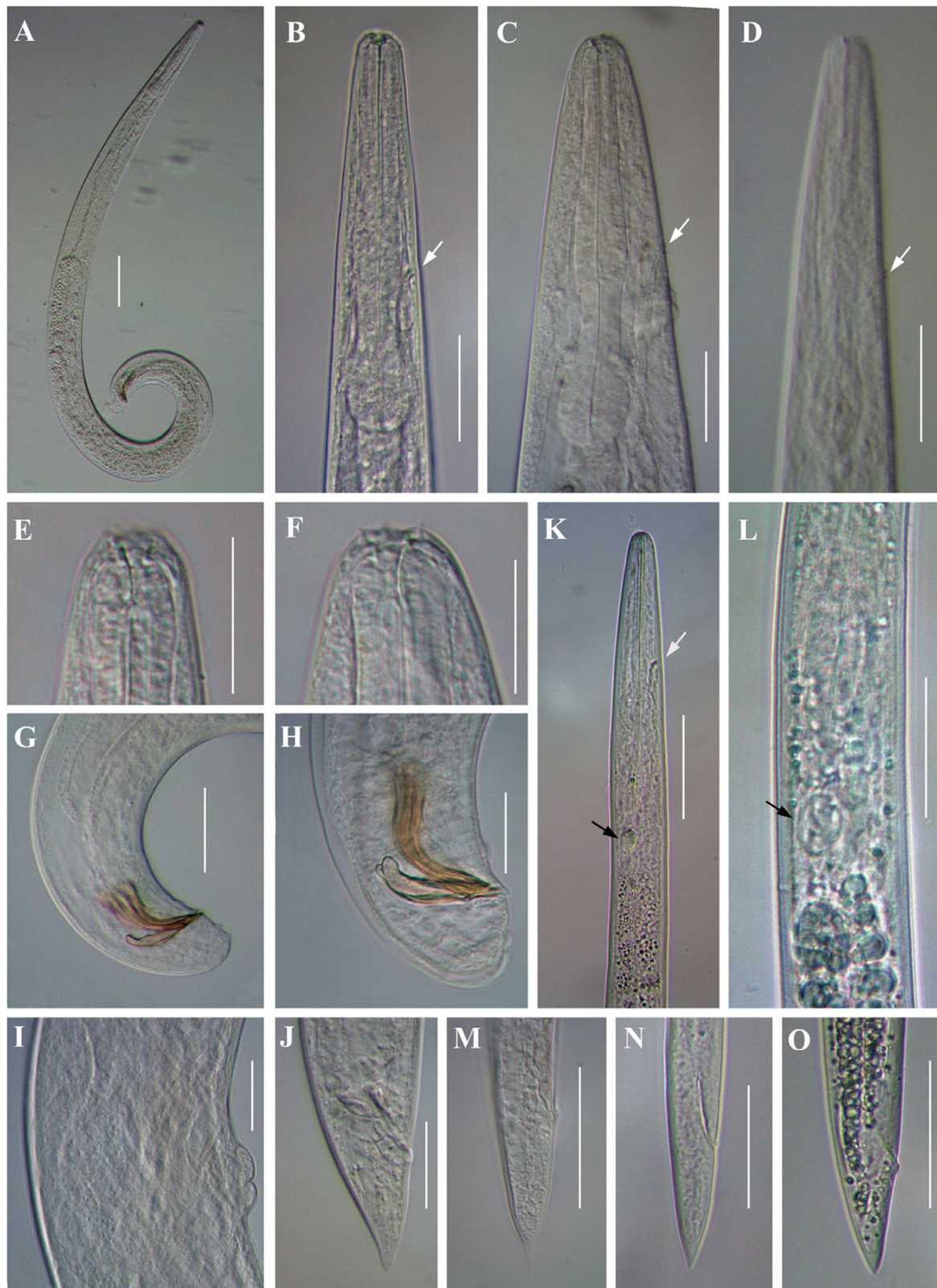
Figure 4. Light microscope micrographs of second-generation adults and infective juvenile (IJ) of *Steinernema tarimense* n. sp. A: Entire body of male; B–D: Stoma and pharynx region of male female and IJ, respectively; E, F: Stoma and pharynx region of male and female, respectively; G, H: Posterior end of male; I: Vulval region of female; J: Posterior end of female; K: Anterior body of IJ; L: Pharynx and intestine junction region of IJ; M, N: Posterior end of fixed IJ; O: Posterior end of fresh IJ. White arrow pointing the excretory pore, black arrow pointing the bacteria sac. Scale bars: A = 100 μm; B–D, G-K, M–O = 50 μm; E, F, L = 25 μm.
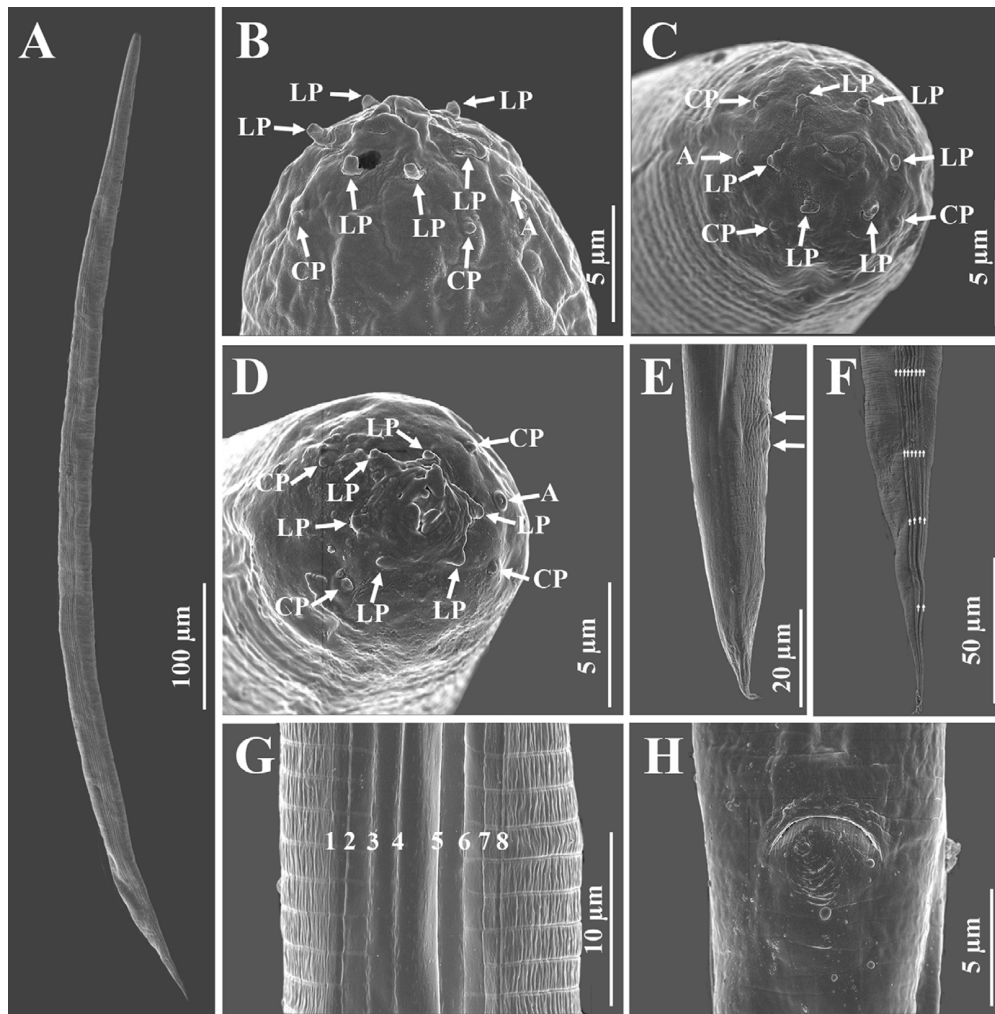
Figure 5. Scanning electron microscope micrographs of infective juveniles of *Steinernema tarimense* n. sp. A: Entire body; B–D: Lip region; E: Tail in lateral view, showing anus and caudal pailla by arrow, respectively; F: Lateral field at tail region, incisures indicated by arrows; G: Lateral field at mid-body, incisures indicated by number 1–8; H: Anus in ventral view. (Abbreviations: A = amphid; CP = cephalic papilla; LP = labial papilla)

S. tarimense n. sp. represents an important addition to our understanding of EPN biodiversity and biogeography in China.

Although *S. tarimense* n. sp. exhibited relatively low similarity in ITS, 28S, and *mt12S* sequences compared to other known *Steinernema* species (Table 4), phylogenetic analyses consistently placed it within an evolutionary clade containing the 'kushidai-clade' members (*S. akhursti*, *S. anantnagense*, *S. kushidai*, and *S. populi*). These taxa collectively formed a well-supported 'feltiae-kushidai-clade' with members of the 'feltiae-clade'. Morphological diagnosis clearly distinguished *S. tarimense* n. sp. from its closest phylogenetic relatives in the 'kushidai-clade'. Comparative morphometrics of both infective juveniles (Table 2) and first-generation males (-Table 3) further confirmed its distinctiveness from other members of the 'feltiae-kushidai-clade'. The combined evidence from comprehensive morphological characterization, detailed morphometric analyses, and robust phylogenetic reconstruction unequivocally supports the recognition of *S. tarimense* as a novel species within the genus *Steinernema*.

Steinernema tarimense n. sp. presented several distinctive biological characters compared to congeners. Notably,

G. mellonella larvae infested with *S. tarimense* n. sp. displayed light black or nearly colorless cadavers, contrasting sharply with the reddish coloration induced by *S. populi* (Figure 6A). The new species demonstrates accelerated developmental rates. Infective juveniles (IJs) and other developmental stages emerged in water within 5–6 days post-infestation (Figure 6B), compared to 10–15 days for *S. populi* (Tian *et al.* 2022). First-generation adults appeared in cadavers within 2–3 days, followed by second-generation adults at 5–6 days, whereas *S. akhursti* required 3–4 days and 7–8 days, respectively (Qiu *et al.* 2005). The unique biological traits observed in the new species likely represent evolutionary adaptations responsed to the extreme environment of its native habitat – the *Populus euphratica* forests along the Tarim River. This region is characterized by aridity, low precipitation, nutrient-poor soils, and limited insect host availability. To survive under these environmental constraints, *S. tarimense* n. sp. appears to have evolved a suite of adaptive traits through natural selections: 1) rapid development by optimizing reproduction within narrow temporal windows; 2) high biomass conversion efficiency by utilizing all host tissues except
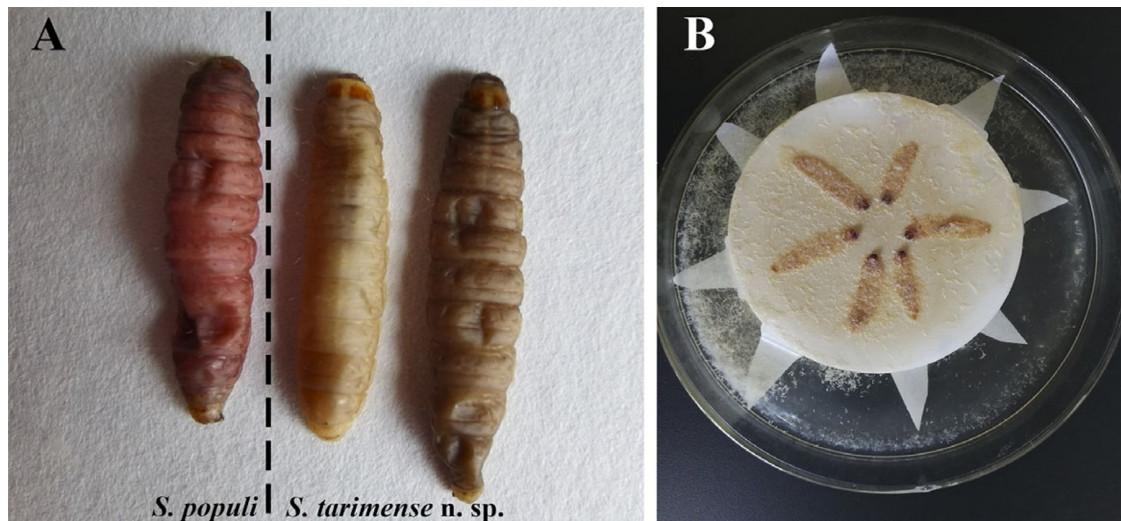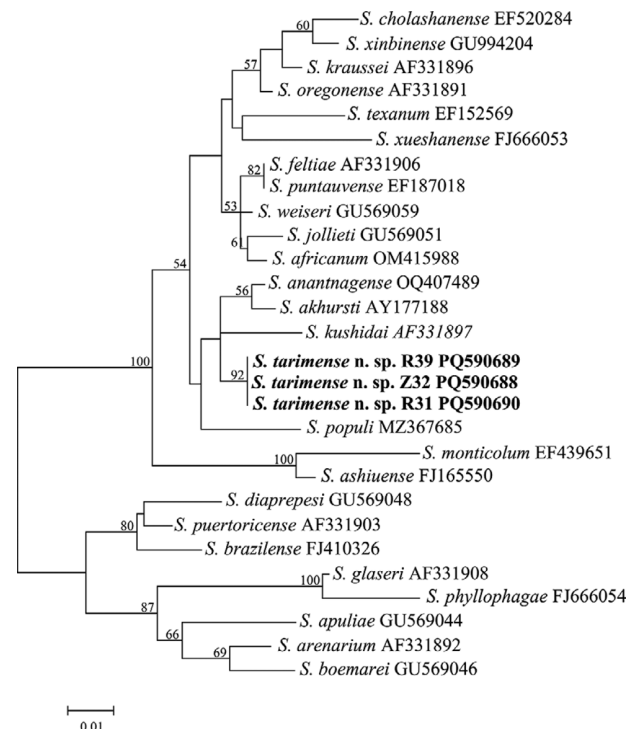
Figure 6. Infection of *Steinernema* species to *Galleria mellonella* larvae. A: Cadavers of *G. mellonella* larvae infested with *S. populi* and *S. tarimense* n. sp. isolate Z32, respectively; B: Third-stage infective juveniles of *S. tarimense* n. sp. migrated out from cadavers.
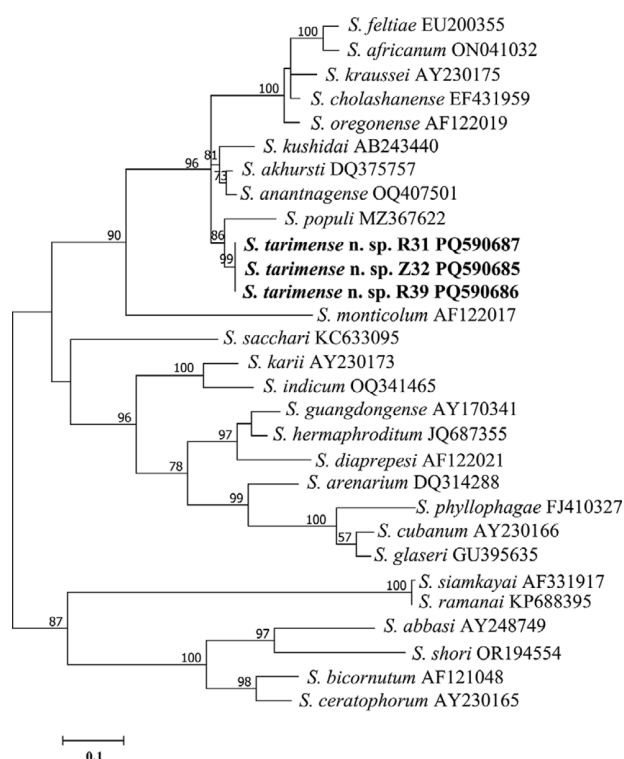
Figure 7. Bayesian 50% majority-rule consensus tree was inferred from the ITS rRNA sequences of *Steinernema tarimense* n. sp., utilizing the GTR + F + G4 model. Bayesian posterior probabilities (PPs) exceeding 50% are indicated for relevant clades. The scale bar represents the number of nucleotide substitutions per site. The new species is indicated in bold.
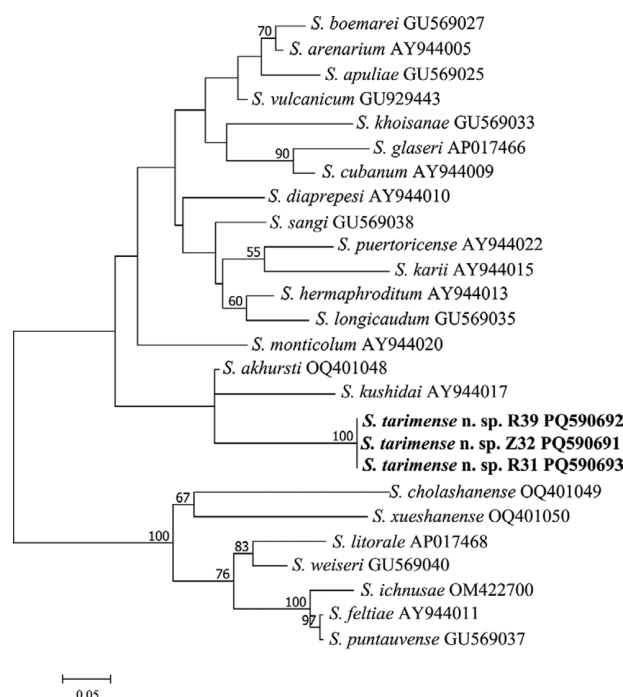

Figure 8. Bayesian 50% majority-rule consensus tree was inferred from the D2D3 regions of 28S rRNA of *Steinernema tarimense* n. sp., utilizing the GTR + F + I + G4 model. Bayesian posterior probabilities (PPs) exceeding 50% are indicated for the relevant clades. The scale bar represents the number of nucleotide substitutions per site. The new species is indicated in bold.

the cuticle; and 3) ecological opportunism by maximizing population persistence despite resource limitations. These traits collectively enhanced the fitness of *S. tarimense* n. sp. in an ecosystem where parasitic opportunities were ephemeral and unpredictable.

Conclusions

Integrated morphological and molecular analyses confirmed *Steinernema tarimense* n. sp. as a new taxon within the genus. The species demonstrates remarkable thermobiological efficiency, with its infective juveniles completing development at 25°C significantly

Figure 9. Bayesian 50% majority-rule consensus tree was inferred for the *mt12S* gene of *Steinernema tarimense* n. sp. using the GTR + F + I + G4 model. Bayesian posterior probabilities (PPs) exceeding 50% are provided for the relevant clades. The scale bar represents the number of nucleotide substitutions per site. The new species is indicated in bold.

faster than related species (*S. cholashanense*, *S. feltiae*, *S. litorale*, and *S. populi*). As the first EPN species described from Xinjiang region, this discovery expands the known biogeographic distribution of *Steinernema* in Asia, represents a valuable indigenous resource for biological control programs in arid ecosystems, and provides novel genetic material for studying thermal adaptation in EPNs.

Supplementary material. The supplementary material for this article can be found at http://doi.org/10.1017/S0022149X25100448.

Competing interests. None.

Ethical standard. The authors assert that all procedures contributing to this work comply with the ethical standards of the relevant national and institutional guides on the care and use of laboratory animals.

References

Bedding RA and Akhurst RJ (1975) A simple technique for the detection of insect parasitic rhabditid nematodes in soil. *Nematologica* **21**, 109–110.

Bhat AH, **Machado RAR**, **Abolafia J**, **Askary THH H H**, **Pŭža V**, **Ruiz-Cuenca AN**, **Rana A**, **Sayed S and Al-Shuraym LA** (2023). Multigene sequence-based and phenotypic characterization reveals the occurrence of a novel entomo-pathogenic nematode species, Steinernema anantnagense *n. sp.* Journal of Nematology **55**, e2023–1.

Bhat AH, **Chaubey AK and Askary TH** (2020) Global distribution of entomo-pathogenic nematodes, *Steinernema* and *Heterorhabditis. Egyptian Journal of Biological Pest Control* **30**, 31.

Chen S, **Li X**, **Yan A**, **Spiridonov SE and Moens M** (2006) A new entomo-pathogenic nematode, *Steinernema hebeiense* sp. n. (Rhabditida, Steinerne-matidae) from North China. *Nematology* **8**, 563–574.

Fallet P, **Gianni L**, **de Machado RAR**, **Bruno P**, **Bernal JS**, **Karangwa P**, **Kajuga J**, **Waweru B**, **Bazagwira D and Degen T** (2022) Comparative screening of Mexican, Rwandan and commercial entomopathogenic nema-todes to be used against invasive fall armyworm, *Spodoptera frugiperda. Insects* **13**, 205.

Hall TA (1999) BioEdit: A user-friendly biological sequences aligenment editor and analysis program for Windows 95/98/NT. *Nucleic Acids Symposium Series* **41**, 95–98.

Kajuga J, **Hategekimana A**, **Yan X**, **Waweru BW**, **Li H**, **Li K**, **Yin J**, **Cao L**, **Karanja D and Umulisa C** (2018) Management of white grubs (Coleoptera: Scarabeidae) with entomopathogenic nematodes in Rwanda. *Egyptian Journal of Biological Pest Control* **28**, 2.

Kalyaanamoorthy S, **Minh BQ**, **Wong TKF**, **von Haeseler A and Jermiin LS** (2017) ModelFinder: Fast model selection for accurate phylogenetic estimates. *Nature Methods* **14**, 587–589.

Koppenhöfer AM, **Shapiro-Ilan DI and Hiltpold I** (2020) Entomopathogenic nematodes in sustainable food production. *Frontiers in Sustainable Food Systems* **4**, 125.

Lacey LA and Georgis R (2012) Entomopathogenic nematodes for control of insect pests above and below ground with comments on commercial pro-duction. *Journal of Nematology* **44**, 218–225.

Large B and Simon DL (1999) Markov Chain Monte Carlo algorithms for the Bayesian analysis of phylogenetic trees. *Molecular Biology and Evolution* **16**, 750–759.

Lis M, **Sajnaga E**, **Skowronek M**, **Wiater A**, **Rachwał K and Kazimierczak W** (2021) *Steinernema sandneri* n. sp. (Rhabditida, Steinernematidae), a new entomopathogenic nematode from Poland. *Journal of Nematology* **53**, e2021–51.

Liu J and Berry RE (1996) *Steinernema oregonensis* n. sp. (Rhabditida, Stei-nernematidae) from Oregon, U.S.A. *Fundamental and Applied Nematology* **19**, 375–380.

Ma J, **Chen S**, **Li X**, **Han R**, **Khatri-Chhetri HB**, **De Clercq P and Moens M** (2012a) A new entomopathogenic nematode, *Steinernema tielingense* n. sp. (Rhabditida, Steinernematidae), from north China. *Nematology* **14**, 321–338.

Ma J, **Chen S**, **De Clercq P**, **Waeyenberge L**, **Han R and Moens M** (2012b) A new entomopathogenic nematode, *Steinernema xinbinense* n. sp. (Nematoda, Steinernematidae), from north China. *Nematology* **14**, 723–739.

Malan AP, **Knoetze R and Tiedt LR** (2016) *Steinernema nguyeni* n. sp. (Rhab-ditida, Steinernematidae), a new entomopathogenic nematode from South Africa. *Nematology* **18**, 571–590.

Mamiya Y (1988) *Steinernema kushidai* n. sp. (Nematoda: Steinernematidae) associated with scarabaeid beetle larvae from Shizuoka, Japan. *Applied Ento-mology and Zoology* **23**, 313–320.

Miller MA, **Pfeiffer W and Schwartz T** (2010) Creating the CIPRES science gateway for inference of large phylogenetic trees. In *Proceedings of the Gateway Computing Environments Workshop* (GCE) LA, New Orleans, LA, USA, 14 November 2010. Piscataway, NJ: Institute of Electrical and Electronics Engineers, 1–8.

Mrácek Z, **Sturhan D and Reid A** (2003) *Steinernema weiseri* n. sp. (Rhabditida, Steinernematidae), a new entomopathogenic nematode from Europe. *Sys-tematic Parasitology* **56**, 37–47.

Mrácek Z, **Liu Q-Z and Nguyen KB** (2009) *Steinernema xueshanense* n. sp. (Rhabditida, Steinernematidae), a new species of entomopathogenic nema-tode from the province of Yunnan, southeast Tibetan Mts., China. *Journal of Invertebrate Pathology* **102**, 69–78.

Nadler SA, **Bolotin E and Stock SP** (2006) Phylogenetic relationships of *Steinernema* Travassos, 1927 (Nematoda, Cephalobina, Steinernematidae) based on nuclear, mitochondrial and morphological data. *Systematic Para-sitology* **63**, 159–179.

Nguyen KB (2007a) Methodology, morphology and identification. In Nguyen KB and Hunt DJ (eds), *Entomopathogenic Nematodes, Systematics, Phylogeny and Bacterial Symbionts*. Nematology Monographs and Perspectives, vol. **5**. Leiden, the Netherlands: Brill, 59–119.

Nguyen KB (2007b) Steinernematidae, species descriptions. In Nguyen KB and Hunt DJ (eds), *Entomopathogenic Nematodes, Systematics, Phylogeny and Bacterial Symbionts*. Nematology Monographs and Perspectives, vol. **5**. Leiden, the Netherlands: Brill, 121–609.

Nguyen KB, **Stuart RJ**, **Andalo V**, **Gozel U and Rogers ME** (2007) *Steinernema texanum* n. sp. (Rhabditida, Steinernematidae), a new entomopathogenic nematode from Texas, USA. *Nematology* **9**, 379–396.

Nguyen KB, **Pŭža V and Mrácek Z** (2008) *Steinernema cholashanense* n. sp. (Rhabditida, Steinernematidae) a new species of entomopathogenic nematode from the province of Sichuan, Chola Shan Mountains, China. *Journal of Invertebrate Pathology* **97**, 251–264.

Nguyen L-T, **Schmidt HA**, **von Haeseler A and Minh BQ** (2015) IQ-TREE: A fast and effective stochastic algorithm for estimating Maximum-Likelihood phylogenies. *Molecular Biology and Evolution* **32**, 268–274.

Nurashikin-Khairuddin W, **Abdul-Hamid SNA**, **Mansor MS**, **Bharudin I**, **Othman Z and Jalinas J** (2022) A Review of entomopathogenic nematodes as a biological control agent for red palm weevil, *Rhynchophorus ferrugineus* (Coleoptera: Curculionidae). *Insects* **13**, 245.

Phan KL, Nguyen NC and Moens M (2001) *Steinernema sangi* sp. n. (Rhabditida, Steinernematidae) from Vietnam. *Russian Journal of Nematology* **9**, 1–7.

Pŭža V, **Nermuť J**, **Konopická J and Habuštová OS** (2024) The effect of *Xenorhabdus* bacteria metabolites on Colorado potato beetle (*Leptinotarsa decemlineata*) adult feeding and larval survival. *Journal of Invertebrate Pathology* **203**, 108075.

Qiu L, **Hu X**, **Zhou Y**, **Mei S**, **Nguyen KB and Pang Y** (2005) *Steinernema akhursti* n. sp. (Nematoda: Steinernematidae) from Yunnan, China. *Journal of Invertebrate Pathology* **90**, 151–160.

Rambaut A (2016) FigTree v1.4.3. Accessed January 2025. Available at http://tree.bio.ed.ac.uk/software/figtree/

Ronquist F, **Teslenko M**, **van der Mark P**, **Ayres DL**, **Darling A**, **Höhna S**, **Larget B**, **Liu L**, **Suchard MA and Huelsenbeck JP** (2012) MrBayes 3.2: Efficient Bayesian phylogenetic inference and model choice across a large model space. *Systematic Biology* **61**, 539–542.

San-Blas E (2013) Progress on entomopathogenic nematology research: a bibliometric study of the last three decades: 1980–2010. *Biological Control* **66**, 102–124.

Spiridonov SE and Subbotin SA (2016) Phylogeny and phylogeography of *Heterorhabditis* and *Steinernema*. In *Advances in Entomopathogenic Nematode Taxonomy and Phylogeny*, vol. **12**. Leiden, The Netherlands: Brill, 413–427.

Spiridonov SE, **Krasomil-Osterfeld K and Moens M** (2004) *Steinernema jollieti* sp. n. (Rhabditida,Steinernematidae), a new entomopathogenic nematode from the American midwest. *Russian Journal of Nematology* **12**, 85–95.

Stokwe NM, **Malan AP**, **Nguyen KB**, **Knoetze R and Tiedt L** (2011) *Steinernema citrae* n. sp. (Rhabditida, Steinernematidae), a new entomopathogenic nematode from South Africa. *Nematology* **13**, 569–587.

Stuart RJ, **Barbercheck ME**, **Grewal PS**, **Taylor RAJ and Hoy CW** (2006) Population biology of entomopathogenic nematodes: concepts, issues, and models. *Biological Control* **38**, 80–102.

Sturhan D, **Spiridonov SE and Mráček Z** (2005) *Steinernema silvaticum* sp. n. (Rhabditida, Steinernematidae), a new entomopathogenic nematode from Europe. *Nematology* **7**, 227–241.

Tarasco E, **Mráček Z**, **Nguyen KB and Triggiani O** (2008) *Steinernema ichnusae* sp. n. (Nematoda, Steinernematidae) a new entomopathogenic nematode from Sardinia Island (Italy). *Journal of Invertebrate Pathology* **99**, 173–185.

Tian C, **Zhu F**, **Li X**, **Zhang J**, **Pŭža V**, **Shapiro-Ilan D**, **Zhao D**, **Liu JW**, **Zhou JJ**, **Ding Y**, **Wang JC**, **Ma J**, **Zhu XF**, **Li MH and Li J** (2022) *Steinernema populi* n. sp. (Panagrolaimomorpha, Steinernematidae), a new entomopathogenic nematode species from China. *Journal of Helminthology* **96**, e57.

Uribe-Lorío L, **Mora M and Stock SP** (2007) *Steinernema costaricense* n. sp. and *S. puntauvense* n. sp. (Rhabditida, Steinernematidae), two new entomopathogenic nematodes from Costa Rica. *Systematic Parasitology* **68**, 167–182.

van Zyl C and Malan AP (2014) The role of entomopathogenic nematodes as biological control agents of insect pests, with emphasis on the history of their mass culturing and in vivo production. *African Entomology* **22**, 235–249.

Vrain TC, **Wakarchuk DA**, **Levesque AC and Hamilton RI** (1992) Intraspecific rDNA restriction fragment length polymorphisms in the *Xiphinema americanum* group. *Fundamentals in Applied Nematology* **15**, 563–574.

White GF (1927) A method for obtaining infective nematode larvae from cultures. *Science* **66**, 302–303.

Wouts W, **Mracek MZ**, **Gerdin S and Bedding RA** (1982) *Neoaplectana* Steiner, 1929 a junior synonym of *Steinernema* Travassos, 1927 (Nematoda: Rhabditida). *Systematic Parasitology* **4**, 147–154.

Yan X, **Waweru B**, **Qiu X**, **Hategekimana A**, **Kajuga J**, **Li H**, **Edgington S**, **Umulisa C**, **Han R and Toepfer S** (2016) New entomopathogenic nematodes from semi-natural and small-holder farming habitats of Rwanda. *Biocontrol Science and Technology* **26**, 820–834.

Yoshida M (2004) *Steinernema litorale* n. sp. (Rhabditida, Steinernematidae), a new entomopathogenic nematode from Japan. *Nematology* **6**, 819–838.